Chapter 1

Motivation and Introduction

1.1 Summary

Considering the growing evidence that CO_2 emissions from fossil fuels are a major contributor to anthropogenic global climate change, a source of carbon-neutral energy will be needed at the scale of our current global energy consumption. We propose to use solar energy due to its abundance and wide availability, but there are significant challenges to producing cost-competitive solar energy solutions. One strategy to reduce the cost of current solar cells is to decouple the directions of light absorption and charge carrier collection by using materials with highly structured junctions. This principle has been shown to improve the efficiency of low-quality—and therefore inexpensive—materials in simulations, but there are significant challenges and drawbacks associated with using highly structured materials. Some of these include the expected increase in surface and junction recombination, as well as the expected decrease in open circuit voltage due to reduced carrier flux per unit of junction area. The use of semiconductor/liquid junctions provides a robust method of forming highly structured junctions and thus allow the expected challenges to be probed in a controlled fashion. These principles form the foundation of the work carried out in this thesis.

1.2 Global Climate Change

The primary motivational force behind this work thesis is the apparent onset of anthropogenic global climate change. Evidence is mounting that human actions have created circumstances in which the energy flux of the Earth is slightly out of balance, causing a rise in the global average temperature, and climate models predict that this temperature change may bring with it a host of sweeping changes in the weather patterns and coastlines of the world. The increased levels of CO_2 and other greenhouse gases in the atmosphere are key contributors to global climate change, and the chief source of CO_2 emissions is the burning of fossil fuels for energy. As a result, finding carbon-neutral alternatives to fossil fuels is an important and active area of research across the sciences, and the focus of this thesis work has been on the understanding and development of silicon devices for solar energy generation.

1.2.1 Radiative Forcing and Warming

When examining the factors contributing to global climate change, it is useful to consider the radiative forcing (RF) associated with each. Radiative forcing is related to the change in energy flux into and out of the Earth's atmosphere, calculated after accounting for thermal equilibration of the stratosphere (upper atmosphere).[1] The RF is measured relative to the preindustrial era (1750), so it primarily represents the changes due to industrialization.[1] Radiative forcing is expected to be generally related to warming and cooling (positive forcing for warming and negative forcing for cooling), but there are many factors affecting the global climate, and sophisticated climate models are needed to predict the precise impact of a given RF on the Earth's temperature.[1] Nevertheless,

radiative forcing is a useful concept because it captures the essence of the climate change problem—that there is an imbalance between the flux of energy into the Earth's atmosphere and out of it. Radiative forcing is also a measurable quantity and therefore independent of global climate models, so that it can be used to assess the likely relative impact of certain conditions without resorting to modeling. As a result, RF is usually discussed in the context of comparing the relative impact of different contributors to global climate change.

The key motivation for moving away from fossil fuels and other sources of CO_2 is the expected impact of increased CO_2 concentrations on global climate change. Figure 1.1 shows the radiative forcing values associated with different human and natural activities.[1] Note that the expected RF due to CO_2 emissions is positive (indicating warming) and larger than all of the other long-lived greenhouse gases combined. Furthermore, note that expected total RF for all human activities is roughly equal to that of CO_2 alone. These observations imply that mitigation of CO_2 emissions would be likely to have a stronger impact on global climate change than any other effort. Figure 1.1 also shows that CH_4, N_2O, and halocarbons make a significant positive contribution to RF, and most of these are not a direct result of burning fossil fuels. Thus, complete mitigation of positive RF induced by humans will necessitate addressing the sources of other long-lived greenhouse gases. Also, there are significant human-induced negative contributions to RF, largely due to aerosols—particulate matter that has been released into the atmosphere.[1] The impact of aerosols on RF begins to illustrate the complexity of anthropogenic global climate change, as both aerosols and CO_2 result from industrial

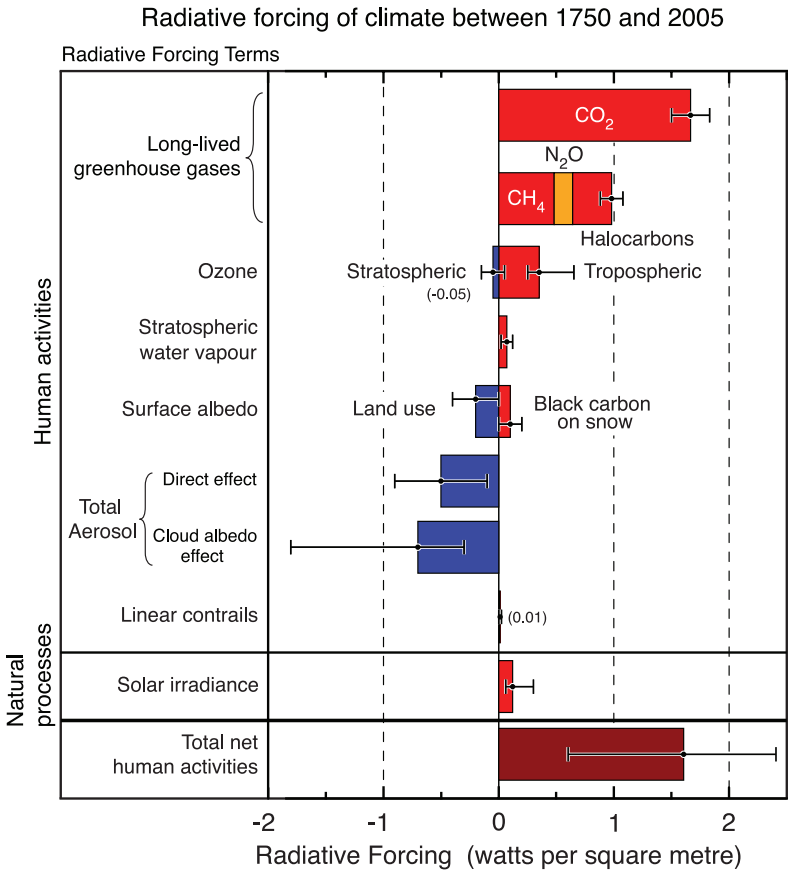

Figure 1.1. *Radiative forcing between 1750 and 2005 (from the IPCC Fourth Assessment Report).[1] Positive forcings are likely to lead to warming while negative forcings are likely to lead to cooling. Note that some contributors (e.g., Surface Albedo) can contribute both positive and negative forcings.*

processes and the burning of fossil fuels, but the effects are in opposing directions. Finally, note that the contribution of natural processes to the RF over this same period of time is expected to be much smaller than those made by human actions.[1] This is compelling evidence for the influence of humans on the observed and predicted global climate change.

Although the impact of radiative forcing on the global average temperature requires climate modeling, changes over the last few years already show a warming trend. Figure 1.2 shows the recent trend in the annual mean global temperature.[2] We can see from this

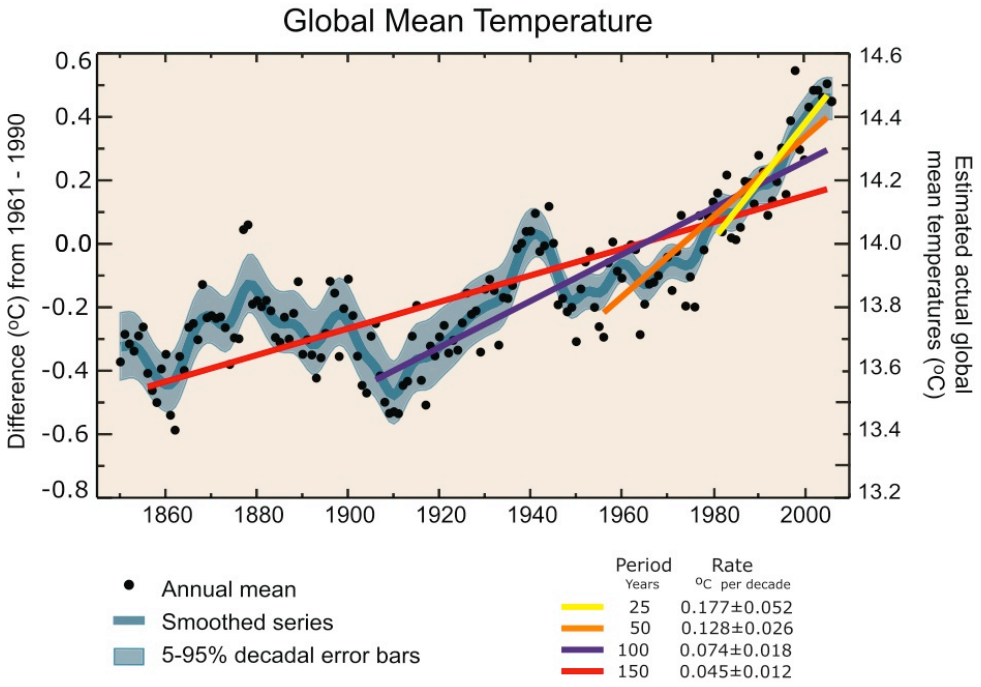

Figure 1.2. *Global average temperature from 1850 to the present (from the IPCC Fourth Assessment Report).[2] Notice that the slope of the temperature increase is rising in recent years, in agreement with the increase in radiative forcing.*

plot that there is a general trend of warming on a global average, although the variation from year to year is quite large. Also plotted are lines showing the averaged behavior over several time periods, and it is immediately apparent that the slopes of these lines are increasing in recent years as compared to the past 150 years.[2] This data does not prove that anthropogenic contributions to radiative forcing are causing an increase in the global temperature, but it does provide an impetus to start reducing the sources of radiative forcing rather than risking the continued increase in global temperature and the subsequent dramatic changes in the global climate. An extremely thorough analysis of the likelihood that global climate change is being caused by human actions, and the probably outcomes of such climate change is available in the Intergovernmental Panel on Climate Change Fourth Assessment Report.[3]

1.2.2 Solar Energy

There are a number of possible choices to replace fossil fuels, but light from the sun is one of the most abundant sources of carbon-neutral energy available.[4] Indeed, the fossil fuels currently used are essentially concentrated energy from the sun stored as chemical bonds. To understand the scale of the available solar energy resource, consider that the solar constant, the energy of incoming sunlight per unit area, is 1.37 kW m^{-2}.[5] The cross-sectional area of the Earth is about 1.27×10^{14} m^2 on average, giving a total incident power from the sun of about 174,000 TW.[5] This is the flux outside the atmosphere of the Earth, so it must be corrected for the total amount of energy that is reflected, which is known as the Earth's albedo and is about 30% on average.[6] This gives a total absorbed power from the sun of about 122,000 TW. This is a vast resource compared to the total global power consumption of only 15 TW currently. Taking this analysis one step further, we can calculate the total land area necessary to generate all of the world's power from the sun. Assuming 10% efficient energy conversion, and given that land mass accounts for only 29.2% of the total surface of the Earth,[5] we find that 0.4% of the Earth's land area would be needed to be covered in solar energy conversion devices in order to power the planet. In contrast, using all of the arable land to grow crops for biomass would only yield a power equivalent of ~8 TW, about half of what is currently being consumed, and there would also be fierce competition between land use for energy crops and for food crops.[4] Thus, solar energy is clearly an attractive avenue for providing significant carbon-neutral energy.

1.3 High Aspect Ratio Structures for Solar Energy

In order to take advantage of the vast solar energy resource in a meaningful way, it will be necessary to develop and manufacture solar energy conversion devices that are cost competitive with fossil fuels and nuclear fission. Although the price of conventional crystalline and multicrystalline silicon solar cells continues to drop due to advances in manufacturing and due to economies of scale,[4] a significant breakthrough in solar energy capture and conversion could lead to a step change in the cost of solar electricity. Furthermore, many groups are vigorously working toward the ultimate goal of a photoelectrochemical fuel-producing device that could be manufactured cheaply at scale. Photon capture and conversion will be an essential component of either photovoltaic or photoelectrochemical energy conversion devices. For these reasons, this work focuses primarily on the photoelectrochemical properties of high-aspect-ratio silicon structures with the goal of understanding the utility of these types of structures for low-cost solar energy capture and conversion.

1.3.1 Decoupling Carrier Collection and Light Absorption

One strategy for mitigating the cost associated with traditional photovoltaics is to enable the use of cheaper materials in the light absorber. In traditional silicon solar cells, the cost of the pure single crystalline silicon typically contributes around 50% of the total module cost,[7] so the impact of using low-cost materials would be significant. However, low-cost semiconductor materials typically suffer from low minority carrier diffusion lengths, leading to inefficient devices due to decreased carrier collection.[8] Since the typical figure of merit used to assess the economic viability of solar modules is the cost

per peak installed watt ($/$W_p$), there is no benefit in sacrificing efficiency (which reduces W_p) in order to reduce the module cost. Thus, strategies must be pursued that maintain high efficiency in inexpensive materials.

One strategy that has been proposed to increase the efficiency of cells constructed from low-cost and low-quality materials is the orthogonalization of light absorption and charge carrier collection (Figure 1.3). In the traditional planar cell, the direction of light

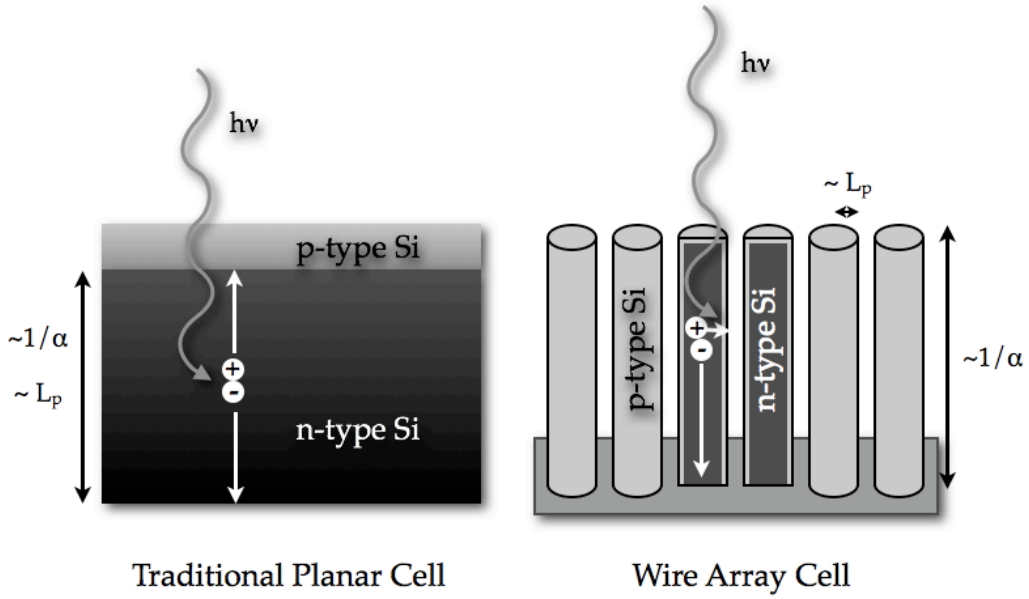

Figure 1.3. *Schematic diagram of a traditional planar solar cell and the proposed wire array geometry. In the planar cell, the absorption length (~1/α) must be comparable to the minority carrier diffusion length (L_p). However, in the wire array cell, the directions of light absorption and minority carrier collection are decoupled, allowing L_p to be independent of 1/α.*

absorption is the same as that of charge carrier collection. Thus, to build an efficient cell, the absorber must be thick enough to absorb all the light (about 100 μm for Si),[9,10] but then the minority carrier diffusion length must be long enough that all of the generated charges are collected. This constraint couples the material absorption to the material purity, typically requiring high purity for indirect semiconductors such as Si.[9] In the

radial junction wire geometry depicted in Figure 1.3, however, the light is still absorbed along the long axis of the wires, while the minority charge carriers can be collected radially. In this case, we expect from an intuitive analysis to be able to build structures from low diffusion length materials while maintaining high efficiencies.

In order to more fully understand the potential benefits and drawbacks of building wire array solar cells, Brendan Kayes carried out detailed 1D diffusion/drift calculations on both planar and radial junction structures.[11] These calculations assumed an abrupt p-n junction, with a p-type base and heavily doped n-type emitter. Furthermore, carrier diffusion along the axis of the wire was not considered in the radial junction case, so that solely radial diffusion was assumed. Under these assumptions, the efficiency surfaces shown in Figure 1.4 were observed.[11] In these simulations, the wire radius was taken to be equal to the minority carrier diffusion length, as this was found to be approximately optimal.[11] The simulations show that, in the absence of traps in the depletion region,

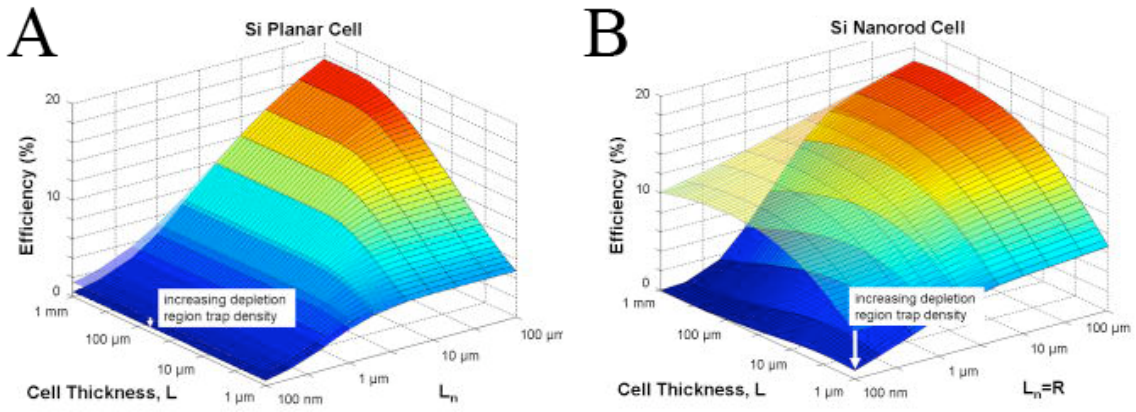

Figure 1.4. *Device physics modeling of the efficiency of planar and wire solar cells.[11] Cell thickness is in the direction of the incident light. A) Traditional planar cell. Note that depletion region recombination has little effect on the observed efficiency. B) Si wire cell. The top curve assumes a low trap density in the depletion region, while the bottom curve assumes uniform trap density throughout the wire. The wire radius is set equal to the minority carrier diffusion length.*

efficiencies in excess of 10% are theoretically possible even for materials with diffusion lengths as low as 100 nm (Figure 1.4B, top curve). However, when the trap density in the depletion region is taken to be equal to that in the quasi-neutral region, the efficiency of the devices is found to drop off sharply at low diffusion lengths (Figure 1.4B, bottom curve). This is to be expected considering the vastly increased depletion area in the very small wires that would need to be employed in materials with low minority carrier diffusion lengths. Nevertheless, there is an area in the 1–10 μm diffusion length regime where an improvement in efficiency is expected with wire array samples over planar samples in the presence of significant depletion region impurities.

Another key consideration arising from simulation of radial junction Si solar cells is the effect of increased junction area on the open circuit voltage (V_{oc}) in the light (Figure 1.5). From Figure 1.5B, it is clear that, even in the absence of significant depletion region recombination, the V_{oc} for a wire array cell is expected to decrease with both

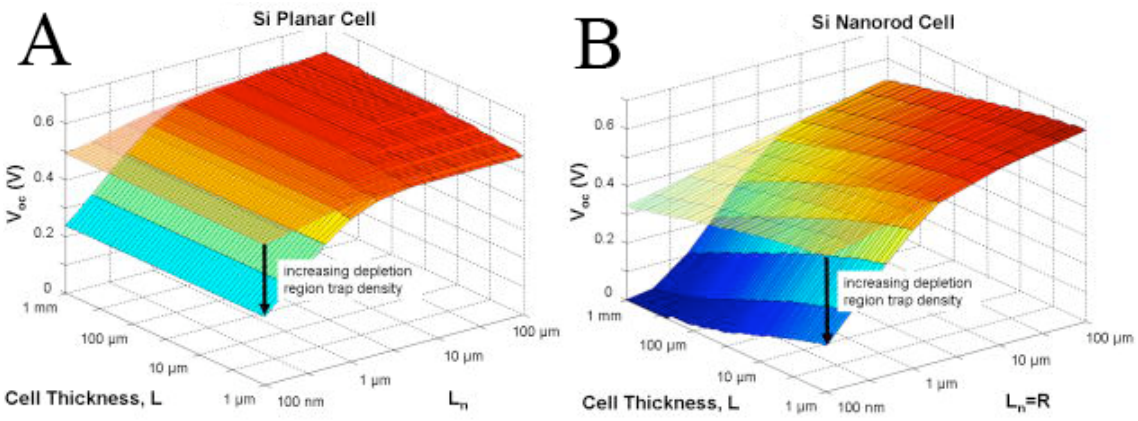

Figure 1.5. *Device physics modeling of the V_{oc} of planar and wire solar cells.[11] Cell thickness is in the direction of the incident light. The top curves assume a low trap density in the depletion region, while the bottom curves assume uniform trap density throughout the wire. A) Traditional planar cell. B) Si wire cell. The wire radius is set equal to the minority carrier diffusion length. Note that the V_{oc} decreases with cell thickness and L_n even in the absence of depletion region recombination.*

decreasing minority carrier diffusion length and decreasing cell thickness.[11] Thus, an increase in the total expected junction area will give rise to a decrease in the observed V_{oc}. This is also expected from a basic analysis of the dependence of V_{oc} on dark and light currents as given for the case in which recombination in the bulk (or quasi-neutral region) is the primary mechanism for recombination:[12]

$$V_{oc} = \frac{AkT}{q} \ln\left(\frac{J_{ph}}{J_0}\right) = \frac{AkT}{q} \ln\left(\frac{I_{ph}}{\gamma I_0}\right), \tag{1.1}$$

where k is Boltzmann's constant, T is the temperature, q is the charge on an electron, A is the diode quality factor, I_{ph} and J_{ph} are the photocurrent and photocurrent density, I_0 and J_0 are the dark current and dark current density, and γ is the surface area enhancement, the ratio of the total junction area to the projected area of the device. Thus, we can see that an increased junction area is expected to predictably lower the value of V_{oc} in the case where the carriers are collected uniformly over the entire junction. This is due to the reduced splitting in the quasi-fermi levels observed when the charge carriers are diluted over a larger junction area.[13-16] In the detailed simulation of Kayes et al. the increase in junction area was convoluted with a decrease in the minority carrier diffusion length,[11] but the analysis based on bulk recombination assumes no such reduction in the diffusion length. Both analyses point to a reduction of about 60 mV in the V_{oc} for every 10-fold increase in junction area relative to projected area. The change in V_{oc} with junction area will be explored primarily in chapters 2 and 3 of this work.

1.3.2 Macroporous Silicon for Physical Model Systems

In the interest of obtaining a more complete understanding of the important factors involved in the design of a highly structured solar cell, physical model systems were initially sought. Macroporous silicon is an excellent candidate for such a model system because it can be readily fabricated from materials of known crystallinity and purity, eliminating the need to simultaneously probe effects originating from the bulk material properties and the structured nature of the junction. Macroporous silicon can be readily fabricated by etching n-type Si in HF containing solutions under illumination from the back of the sample.[17-23] The pore etching typically proceeds in the <100> direction and pore formation is believed to take place primarily under hole-limited conditions, where holes generated at the back of n-type silicon diffuse toward the front and are collected at the pore tips.[17-23]

Samples of n-type porous silicon can then be used as a model system for wire array cells because there is significant potential for the radial diffusion of minority charge carriers and their subsequent collection at a junction formed at the pore sidewalls. By forming semiconductor/liquid junctions with macroporous silicon devices, conformal contact can be made to the pore sidewalls and carriers can be harvested at the sidewalls. Chapters 2 and 3 of this work describe photoelectrochemical experiments conducted on n-type macroporous silicon.

1.3.3 Chemical Vapor Deposition Growth of Wires

Growth of silicon wire arrays by chemical vapor deposition (CVD) is a promising route to the inexpensive, scalable synthesis of structured silicon devices starting from

widely available starting materials. CVD by the vapor-liquid-solid (VLS) method was pioneered by Wagner and Ellis in the 1960s for the growth of Si wires.[24,25] In the VLS method (Figure 1.6), silicon precursors (typically SiH_4 or $SiCl_4$) are introduced in the gas phase in the presence of Au particles. At elevated temperatures, the precursors decompose and Si deposits in the Au particle, eventually forming a liquid eutectic mixture. As the particles become supersaturated with Si, rods begin to grow by precipitation of Si with the Au catalyst particle staying on the tips of the rods. CVD growth of wires by VLS is a promising route for the production of low-cost materials because it can be carried out at large scales, and it can be used to produce structured materials directly.[26-31]

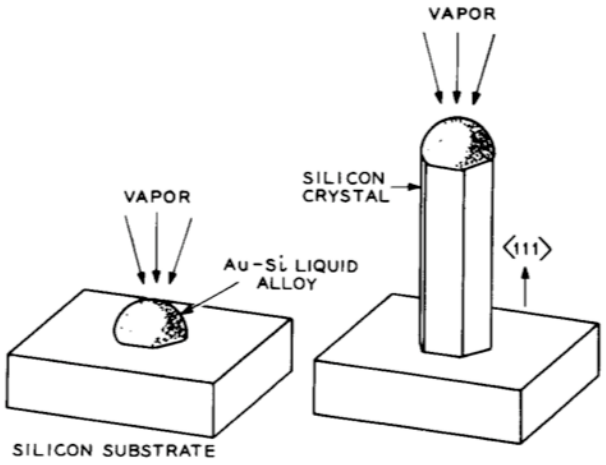

Figure 1.6 *- Schematic of Si wire growth by the CVD-VLS method.[25] Beginning with Au catalyst particles, Si vapor dissolves in the catalyst and then precipitates to form wires that grow preferentially in the <111> direction.*

In particular, work in the Atwater and Lewis groups has demonstrated controlled growth of uniform arrays of Si wires starting from either Au or Cu catalyst particles with $SiCl_4$ as the feed gas.[29] The key to obtaining uniform arrays of Si wires was the use of an oxide barrier layer to prevent flow and pooling of the catalyst at the high temperatures used for growth.[29] It was also found that the as-grown wire arrays could be readily removed from the substrate in a thin film of polymer (e.g. polydimethylsiloxane—PDMS), leaving the ends of the wires exposed for further chemistry and measurement.[32]

Finally, it was demonstrated that although a single crystalline substrate is used for templated growth, that substrate can be used repeatedly by removal of the wires from the surface, selective etching of the wire "stumps," and electrodeposition of additional Au catalyst back into the oxide mask.[30] The demonstration of these remarkable fabrication techniques opens the door to many uses of CVD-grown Si wire arrays in devices for solar energy capture and conversion. Chapters 4 and 5 of this work will focus on the photoelectrochemical results obtained from studying these wire arrays.

1.3.4 Solid State Structured Devices

Before the use of wires for solar energy conversion was explored in the literature, other techniques were explored that made use of reduced carrier collection distances. These include the vertical multijunction solar cell[33] and the parallel multijunction solar cell,[34,35] both of which incorporate significantly increased junction areas with commensurate smaller distances for minority carriers to travel before collection. Furthermore, both methods were shown to produce efficient cells using techniques that give rise to high purity silicon.[36,37] These results strengthen the principle that structured solar cells can be produced, but low-cost fabrication methods need to be pursued in order to realize the full utility of large junction areas.

Other methods have also been employed to produce high aspect ratio solar energy conversion devices that do not involve traditional diffused p-n junctions but that nevertheless produce solar cells with no liquid component. Most of the other devices that have been constructed using structured materials have consisted of semiconductor rods or wires embedded in conducting polymer layers.[38-43] In these cases, the conductive

polymer typically acts as the absorber, with the semiconductor rods serve as both the emitter layer and as charge conduction pathways for the minority carriers after they have been collected.[38-41,43] The principle of increasing junction area in order to improve carrier collection in low diffusion length materials is still at work in these studies, however, as there is an enhanced junction area due to contact with the semiconductor wires. In fact, the most successful polymeric solar cells to date have been fabricated using blends of conductive polymer with fullerene derivatives.[44-47] These bulk heterojunction devices are expected to have very large junction areas, which are necessary due to the short exciton diffusion length in conductive polymers (~10 nm).[48]

There have also been an number of studies employing Si nanowires in recent years. In one study, n-type Si nanowires were grown by CVD-VLS on a multicrystalline p-type Si substrate, thus forming the p-n junction during the wire growth process.[49] In this case the junction is axial rather than radial, so the principle of enhanced junction area does not apply. In another study, p-type Si nanowires were grown by CVD-VLS directly on a thin film of Ta_2N on stainless steel, and the solid state junction was formed by conformal deposition of n-type amorphous Si.[50] Square centimeter sized cells were produced in this case, although both the J_{sc} and V_{oc} were found to be limited by shunting and geometrical considerations.[50] In another study, n-type Si wires were created by chemical etching of a Si wafer, and a thin film of p-type amorphous Si was deposited to form the junction.[51] In this case a significant improvement in J_{sc} was observed compared to previous studies.

1.4 Semiconductor Liquid Junctions

The material presented in this section is intended to set the stage for the photoelectrochemistry conducted in this work, but there are a number of excellent books and reviews available describing both semiconductor physics and semiconductor photoelectrochemistry in detail.[9,12,52,53] As an alternative to making metallurgical p-n junction contacts to the structured samples considered here, semiconductor/liquid junctions were formed. Liquid junctions were used primarily to ensure good conformal contact to all of the structures studied, and those employed here are also known to form high barrier height, low surface recombination velocity junctions with Si.

1.4.1 The n-Si/Methanol Junction

There is a significant body of work in the literature concerning non-aqueous semiconductor/liquid junctions, particularly the Si/methanol junction. For both n- and p-type silicon in contact with methanol containing a series of redox couples with solution potentials that vary over 1 V, it was found that the open circuit voltage (V_{oc}) behavior in the light was nearly ideal.[54,55] This indicates that the fermi-level pinning typically observed in Si/metal contacts is not observed under the appropriate conditions in Si/liquid contacts. This allows the redox couple in the liquid phase to be chosen in order to set the barrier height of the junction. For n-type Si, ferrocene$^{+/0}$ and dimethylferrocene$^{+/0}$ give high barrier height contacts.[54] Furthermore, the n-Si/methanol/ferrocene$^{+/0}$ system has been shown to have good interfacial properties for photoelectrochemistry. Studies of the surface recombination velocity (SRV) of various silicon interfaces showed that the SRV for n-Si while in contact with ferrocene$^{+/0}$/methanol is on the order of 20 cm s^{-1}, which is

comparable to or lower than the value found for Si in HF.[56] Furthermore, this low SRV was retained when the samples were removed into a N_2 atmosphere, which is not the case for samples treated in a ferrocene/THF solution.[56] This was taken to indicate surface functionalization of n-Si in methanol in the presence of a one-electron oxidant, most likely due to the formation of a monolayer of methoxy groups on the Si surface.[56,57]

Given the high barrier heights and low SRV values obtainable, the n-Si/methanol/ ferrocene$^{+/0}$ system is expected to produce excellent photoelectrochemical energy conversion devices. With this system, over 10% energy conversion efficiency was found for single crystalline samples,[58-60] and efficiencies as high as 7.2% were achieved for polycrystalline Si.[61] However, when a liquid is used as the contacting phase rather than a metal or a semiconductor, charge conduction in the liquid will necessarily be due to mass transport of the redox species used. These mass transport limitations will change the shape of the measured *J-E* curves in accordance with the behavior of Nernstian redox molecules—a sigmoidal distortion of the curve is expected near the anodic and cathodic mass-transport-limited currents, and there will be a commensurate shift in the curves, even far away from the limiting currents (Figure 1.7).[62] This gives rise to the concentration overpotential loss in the cell, which can also be considered as the energy used to set up the concentration gradient from the electrode to the bulk of the solution. Since the ferrocenium derivatives are deeply colored, they have typically been present in small amounts for photoelectrochemical measurements, giving rise to a reasonably large concentration overpotential loss. This loss can be measured by tracing out the Nernstian *J-E* curve at a Pt electrode and measuring the cathodic and anodic limiting currents.[62,63]

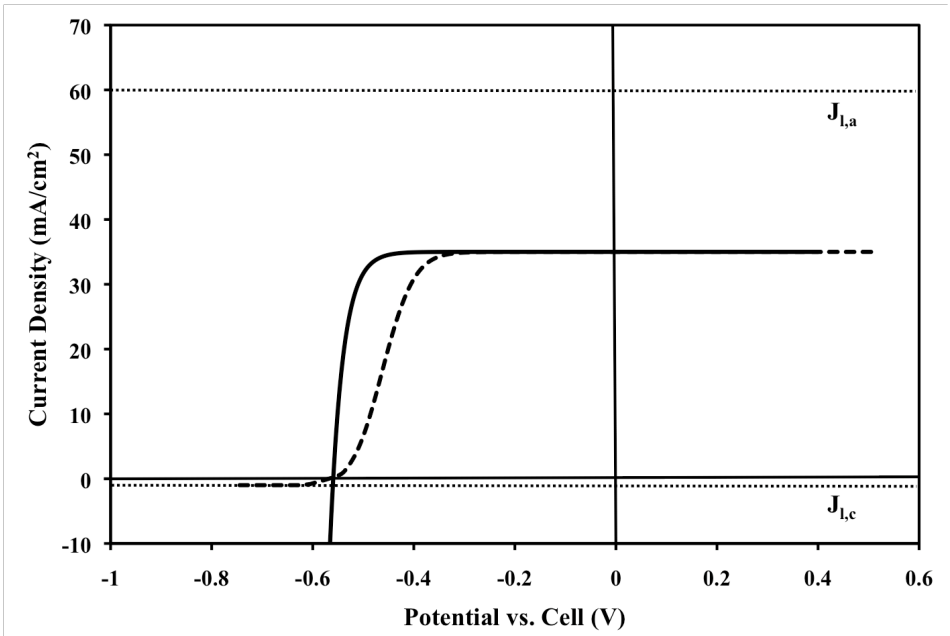

Figure 1.7. *Concentration overpotential effect. The dotted lines indicate the anodic and cathodic mass transport limited currents. The solid line shows a theoretical bulk recombination limited p-n junction photodiode at a typical current density. The dashed line shows the same diode after concentration overpotential has been applied according to the mass transport limited currents. Note that the curve is shifted to more positive potentials even far away from the small cathodic limiting current.*

When the concentration overpotential and series resistances losses are reduced—as they are in a thin layer, two-electrode photoelectrochemical cell—the *J-E* curves for n-type Si show the expected diodic character, and the efficiency values are increased to 14%.[58] Correction for the concentration overpotential and series resistance losses will be an important consideration when measuring structured samples, and this correction is discussed in Chapters 2, 4, and 5 of this work.

1.4.2 Structured Semiconductors in Photoelectrochemical Cells

There are numerous examples of the use of structured semiconductor materials in photoelectrochemical energy conversion devices. Perhaps the most prevalent of such devices is the dye-sensitized solar cell (DSSC) initially developed by Grätzel and O'Regan,[64] which has since been studied extensively, reaching efficiencies greater than

10%.[65-67] The DSSC consists of nanoparticles of TiO_2 or another large band-gap metal oxide sensitized with a dye that absorbs in the visible (Figure 1.8). Upon excitation, the dye can rapidly inject an electron into the TiO_2. The electron travels through the TiO_2 to the back contact, and through the external circuit to a counter electrode, where it can reduce I_3^- to I^-. Finally, the reduced form of the dye is regenerated by reaction with I^-. Thus, the cell is a regenerative photoelectrochemical cell using a structured material, where the structure serves the primary function of increasing the area for dye absorption. DSSCs have been developed in which the metal oxide component consists of oriented arrays of wires,[68-71] but these devices retain the essential elements of nanoparticle DSSCs in that the semiconductor is functioning primarily as a charge collector rather than as the

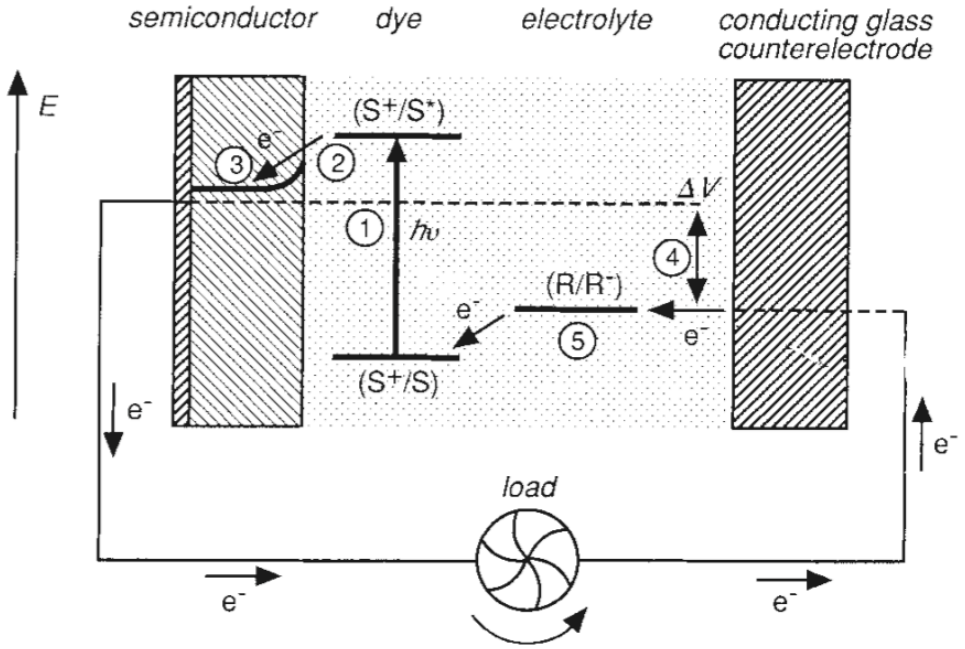

Figure 1.8. *Schematic of the dye-sensitized solar cell.[64] The semiconductor typically consists of nanoparticles of TiO_2. 1) Excitation of the dye by incident light. 2) Charge injection from the dye excited state. 3) Electron transport to the back contact. 4) The expected V_{oc} of the cell is given by the difference shown. 5) The dye is regenerated by a mediator.*

absorber. However, the use of metal oxide wires is also expected to give rise to improvements in the majority carrier charge transport properties of these devices.

There are also examples of using structured semiconductor materials as the main absorber in photoelectrochemical cells. In particular, work by Kelly and co-workers. showed that significant improvements in the charge carrier collection efficiency in GaP could be obtained by subjecting the substrate to porous etching.[72,73] This result directly demonstrates the principle that decoupling the directions of light absorption and charge carrier collection in low-quality semiconductors can lead to improved carrier collection. The use of macroporous Si in this work is analogous to the previous studies by Kelly and co-workers, except that Si can be made routinely with much longer minority carrier diffusion lengths. In addition, recent studies have shown photoelectrochemical measurements on silicon wire arrays produced by CVD-VLS growth[74] and by top-down etching to produce wires.[75]

1.5 Conclusions

The evidence for anthropogenic contributions to radiative forcing, and therefore to global climate change, is overwhelming. In particular, the emissions of CO_2 from the burning of fossil fuels forms a large portion of the radiative forcing, and therefore the elimination of fossil fuels is an excellent target for current research. Furthermore, of the currently available sources of carbon-neutral energy, solar energy is one of the most promising because the incident power from the sun is nearly five orders of magnitude greater than our current global energy consumption. Harvesting this energy requires the widespread deployment of solar energy conversion devices, but the current cost of solar

photovoltaics is too high relative to the cost of fossil fuels to drive this deployment. Therefore, reducing the cost of solar cells and other solar energy conversion devices would have a dramatic impact on global CO_2 emissions.

One strategy for producing inexpensive solar energy conversion devices is to decouple the directions of light absorption and charge carrier collection, thereby allowing the use of low-cost materials that have low minority carrier diffusion lengths. This decoupling can, in theory, be accomplished by producing arrays of semiconductor wires having radial junctions, and simulations have shown that a significant benefit in efficiency should be possible for materials with diffusion lengths in the range of 1-10 μm. Although the efficiency improves under these conditions, it is partially lowered due to an expected loss in V_{oc} with increasing junction area.

Based on the simulation results, there are several fruitful avenues of research. One approach is to use a physical model system, such as macroporous silicon, in which all other factors but the junction geometry are held constant, in order to determine the effect of junction structure on carrier collection and V_{oc}. Demonstrating the efficiency of macroporous silicon samples would also confirm that no other deleterious effects are expected in high junction area devices. The controlled reduction of the minority carrier lifetime in physical model systems would also be a way to demonstrate the principle of decoupling charger carrier collection from light absorption. In addition to physical model systems, working on devices produced by inexpensive techniques, such as CVD, has the potential to show the feasibility of producing low-cost solar energy conversion devices by

using semiconductor wire arrays. These research directions are the primary ones pursued in this thesis and will be discussed in Chapters 2-5.

1.6 References

1. Forster, P.; Ramaswamy, V.; Artaxo, P.; Bernsten, T.; Betts, R.; Fahey, D. W.; Haywood, J.; Lean, J.; Lowe, D. C.; Myhre, G.; Nganga, J.; Prinn, R.; Raga, G.; Schulz, M.; Van Dorland, R., 2007: Changes in Atmospheric Constituents and in Radiative Forcing. *In: Climate Change 2007: The Physical Science Basis. Contribution to Working Group I to the Fourth Assessment Report of the Intergovernmental Panel on Climate Change* [Solomon, S., Qin, D., Manning, M., Chen, Z., Marquis, M., Averyt, K. B., Tignor, M., Miller, H. L. (eds.)]. Cambridge University Press, Cambridge, United Kingdom and New York, NY, USA.
2. Trenberth, K. E.; Jones, P. D.; Ambenje, P.; Bojariu, R.; Easterling, D.; Klein Tank, A.; Parker, D.; Rahimzadeh, F.; Renwick, J. A.; Rusicucci, M.; Soden, B.; Zhai, P., 2007: Observations: Surface and Atmospheric Climate Change. *In: Climate Change 2007: The Physical Science Basis. Contribution of Working Group I to the Fourth Assessment Report of the Intergovernmental Panel on Climate Change* [Solomon, S., Qin, D., Manning, M., Chen, Z., Marquis, M., Averyt, K. B., Tignor, M., Miller, H. L. (eds.)]. Cambridge University Press, Cambridge, United Kingdom and New York , NY, USA.
3. IPCC Fourth Assessment Report - Working Group I Report "The Physical Science Basis", 2007.
4. Sims, R. E. H.; Schock, R. N.; Adegbululgbe, A.; Fenhann, J.; Konstantinaviciute, I.; Moomaw, W.; Nimir, H. B.; Schlamadinger, B.; Torres-Martinez, J.; Turner, C.; Uchiyama, Y.; Vuori, S. J. V.; Wamukonya, N.; Zhang, X., 2007: Energy Supply. *In: Climate Change 2007: Mitigation. Contribution of Wroking Group III to the Fourth Assessment Report of the Intergovernmental Panel on Climate Change* [Metz, B., Davidson, O. R., Bosch, P. R., Dave, R., Meyer, L. A. (eds.)]. Cambridge University Press, Cambridge, United Kingdom and New York, NY, USA.
5. *CRC Handbook of Chemistry and Physics*; 77th ed.; Lide, D. R., Ed.; CRC Press: New York, 1996.

6. Goode, P. R.; Qiu, J.; Yurchyshyn, V.; Hickey, J.; Chu, M. C.; Kolbe, E.; Brown, C. T.; Koonin, S. E. *Geophys. Res. Lett.* **2001**, *28*, 1671-1674.
7. Tao, M., 2008: Inorganic Photovoltaic Solar Cells: Silicon and Beyond. *In: The Electrochemical Society Interface*
8. Schlosser, V. IEEE Trans. Electron Devices **1984**, 31, 610-613.
9. Sze, S. M. *Physics of Semiconductor Devices*; 2nd ed.; John Wiley & Sons: New York, 1981.
10. ASTM Standard G173, 2003e1, "Standard Tables for Reference Solar Spectral Irradiances: Direct Normal and Hemispherical on 37º Tilted Surface," ASTM International, West Conshohocken, PA, 2003, DOI: 10.1520/G0173-03E01.
11. Kayes, B. M.; Atwater, H. A.; Lewis, N. S. *J. Appl. Phys.* **2005**, *97*, 114302.
12. Tan, M. X.; Laibinis, P. E.; Nguyen, S. T.; Kesselman, J. M.; Stanton, C. E.; Lewis, N. S. In *Progress In Inorganic Chemistry, Vol 41*; John Wiley & Sons Inc: New York, 1994; Vol. 41, p 21-144.
13. Kenyon, C. N.; Tan, M. X.; Kruger, O.; Lewis, N. S. *J. Phys. Chem. B* **1997**, *101*, 2850-2860.
14. Kruger, O.; Kenyon, C. N.; Tan, M. X.; Lewis, N. S. *J. Phys. Chem. B* **1997**, *101*, 2840-2849.
15. Tan, M. X.; Kenyon, C. N.; Kruger, O.; Lewis, N. S. *J. Phys. Chem. B* **1997**, *101*, 2830-2839.
16. Tan, M. X.; Kenyon, C. N.; Lewis, N. S. *J. Phys. Chem.* **1994**, *98*, 4959-4962.
17. Lehmann, V. Electrochemistry of Silicon: Instrumentation, Science, Materials and Applications; Wiley-VCH, 2002.
18. Lehmann, V. *Thin Solid Films* **1995**, *255*, 1-4.
19. Lehmann, V.; Stengl, R.; Luigart, A. Mater. Sci. Eng. B-Solid State Mater. Adv. Technol. **2000**, 69, 11-22.
20. Lehmann, V. J. Electrochem. Soc. **1993**, 140, 2836-2843.
21. Lehmann, V.; Grüning, U. *Thin Solid Films* **1997**, *297*, 13-17.
22. Lehmann, V.; Föll, H. *J. Electrochem. Soc.* **1990**, *137*, 653-659.
23. Al Rifai, M. H.; Christophersen, H.; Ottow, S.; Carstensen, J.; Foll, H. *J. Electrochem. Soc.* **2000**, *147*, 627-635.

24. Wagner, R. S.; Ellis, W. C. Transactions of the Metallurgical Society of Aime **1965**, 233, 1053-&.

25. Wagner, R. S.; Ellis, W. C. *Appl. Phys. Lett.* **1964**, *4*, 89-&.

26. Cui, Y.; Lauhon, L. J.; Gudiksen, M. S.; Wang, J. F.; Lieber, C. M. *Appl. Phys. Lett.* **2001**, *78*, 2214-2216.

27. Wu, Y.; Cui, Y.; Huynh, L.; Barrelet, C. J.; Bell, D. C.; Lieber, C. M. *Nano Lett.* **2004**, *4*, 433-436.

28. Lombardi, I.; Hochbaum, A. I.; Yang, P.; Carraro, C.; Maboudian, R. *Chem. Mat.* **2006**, *18*, 988-991.

29. Kayes, B. M.; Filler, M. A.; Putnam, M. C.; Kelzenberg, M. D.; Lewis, N. S.; Atwater, H. A. *Applied Physics Letters* **2007**, 103110-1-3.

30. Spurgeon, J. M.; Plass, K. E.; Kayes, B. M.; Brunschwig, B. S.; Atwater, H. A.; Lewis, N. S. *Appl. Phys. Lett.* **2008**, *93*.

31. Gowrishankar, V.; Miller, N.; McGehee, M. D.; Misner, M. J.; Ryu, D. Y.; Russell, T. P.; Drockenmuller, E.; Hawker, C. J. *Thin Solid Films* **2006**, *513*, 289-294.

32. Plass, K. E.; Filler, M. A.; Spurgeon, J. M.; Kayes, B. M.; Maldonado, S.; Brunschwig, B. S.; Atwater, H. A.; Lewis, N. S. *Adv. Mater.* **2009**, *21*, 325-328.

33. Rahilly, W. P. Record of the Ninth IEEE Photovoltaic Specialists Conference|Record of the Ninth IEEE Photovoltaic Specialists Conference **1972**, 44-52|xii+388.

34. Green, M. A.; Wenham, S. R. *Appl. Phys. Lett.* **1994**, *65*, 2907-2909.

35. Wenham, S. R.; Green, M. A.; Edmiston, S.; Campbell, P.; Koschier, L.; Honsberg, C. B.; Sproul, A. B.; Thorpe, D.; Shi, Z.; Heiser, G. *Sol. Energ. Mat. Sol.* **1996**, *41-2*, 3-17.

36. Wohlgemuth, J.; Scheinine, A. Fourteenth IEEE Photovoltaic Specialists Conference 1980| Fourteenth IEEE Photovoltaic Specialists Conference 1980 **1980**, 151-5|1411.

37. Zheng, G. F.; Wenham, S. R.; Green, M. A. *Progress in Photovoltaics* **1996**, *4*, 369-373.

38. Takanezawa, K.; Hirota, K.; Wei, Q. S.; Tajima, K.; Hashimoto, K. *J. Phys. Chem. C* **2007**, *111*, 7218-7223.

39. Wei, Q. S.; Hirota, K.; Tajima, K.; Hashimoto, K. *Chem. Mat.* **2006**, *18*, 5080-5087.

40. Gur, I.; Fromer, N. A.; Geier, M. L.; Alivisatos, A. P. *Science* **2005**, *310*, 462-465.

41. Huynh, W. U.; Dittmer, J. J.; Alivisatos, A. P. *Science* **2002**, *295*, 2425-2427.

42. Kang, Y. M.; Park, N. G.; Kim, D. *Appl. Phys. Lett.* **2005**, *86*, 113101.

43. Lin, Y. T.; Zeng, T. W.; Lai, W. Z.; Chen, C. W.; Lin, Y. Y.; Chang, Y. S.; Su, W. F. *Nanotechnology (UK)* **2006**, *17*, 5781-5785.

44. Brabec, C. J.; Sariciftci, N. S.; Hummelen, J. C. *Adv. Funct. Mater.* **2001**, *11*, 15-26.

45. Kim, J. Y.; Lee, K.; Coates, N. E.; Moses, D.; Nguyen, T. Q.; Dante, M.; Heeger, A. J. *Science* **2007**, *317*, 222-225.

46. Li, G.; Shrotriya, V.; Huang, J. S.; Yao, Y.; Moriarty, T.; Emery, K.; Yang, Y. *Nat. Mater.* **2005**, *4*, 864-868.

47. Liang, Y.; Wu, Y.; Feng, D.; Tsai, S.-T.; Son, H.-J.; Li, G.; Yu, L. *J Am Chem Soc* **2009**, *131*, 56-7.

48. Haugeneder, A.; Neges, M.; Kallinger, C.; Spirkl, W.; Lemmer, U.; Feldmann, J.; Scherf, U.; Harth, E.; Gugel, A.; Mullen, K. *Phys. Rev. B* **1999**, *59*, 15346-15351.

49. Stelzner, T.; Pietsch, M.; Andra, G.; Falk, F.; Ose, E.; Christiansen, S. *Nanotechnology (UK)* **2008**, *19*.

50. Tsakalakos, L.; Balch, J.; Fronheiser, J.; Korevaar, B. A.; Sulima, O.; Rand, J. *Appl. Phys. Lett.* **2007**, *91*.

51. Garnett, E. C.; Yang, P. D. *J. Am. Chem. Soc.* **2008**, *130*, 9224-+.

52. Lewis, N. S.; Rosenbluth, M. L. In *Photocatalysis: Fundamentals and Applications*; Serpone, N., Pelizzetti, E., Eds.; Wiley Interscience: New York, 1989, p 45-121.

53. Pierret, R. F. *Advanced Semiconductor Fundamentals*; 2nd ed.; Prentice Hall: Upper Saddle River, NJ, 2003; Vol. 6.

54. Lewis, N. S. J. Electrochem. Soc. **1984**, 131, 2496-2503.

55. Rosenbluth, M. L.; Lewis, N. S. *J. Phys. Chem.* **1989**, *93*, 3735-3740.

56. Gstrein, F.; Michalak, D. J.; Royea, W. J.; Lewis, N. S. *J. Phys. Chem. B* **2002**, *106*, 2950-2961.

57. Groner, M. D.; Koval, C. A. *J. Electroanal. Chem.* **2001**, *498*, 201-208.

58. Gibbons, J. F.; Cogan, G. W.; Gronet, C. M.; Lewis, N. S. *Appl. Phys. Lett.* **1984**, *45*, 1095-1097.

59. Gronet, C. M.; Lewis, N. S.; Cogan, G. W.; Gibbons, J. F. *Proc. Natl. Acad. Sci.* **1983**, *80*, 1152-1156.

60. Rosenbluth, M. L.; Lieber, C. M.; Lewis, N. S. *Appl. Phys. Lett.* **1984**, *45*, 423-425.

61. Cogan, G. W.; Gronet, C. M.; Gibbons, J. F.; Lewis, N. S. *Appl. Phys. Lett.* **1984**, *44*, 539-541.

62. Bard, A. J.; Faulkner, L. R. *Electrochemical Methods: Fundamentals and Applications*; 2nd ed.; John Wiley & Sons, Inc.: Hoboken, NJ, 2001.

63. Hamann, T. W.; Gstrein, F.; Brunschwig, B. S.; Lewis, N. S. *J. Am. Chem. Soc.* **2005**, *127*, 7815-7824.

64. Oregan, B.; Gratzel, M. *Nature* **1991**, *353*, 737-740.

65. Gratzel, M.; Kalyanasundaram, K. *Curr. Sci.* **1994**, *66*, 706-714.

66. Hagfeldt, A.; Gratzel, M. *Accounts Chem. Res.* **2000**, *33*, 269-277.

67. Gratzel, M. J. Photochem. Photobiol. C-Photochem. Rev. **2003**, 4, 145-153.

68. Baxter, J. B.; Aydil, E. S. *Appl. Phys. Lett.* **2005**, *86*.

69. Law, M.; Greene, L. E.; Johnson, J. C.; Saykally, R.; Yang, P. D. *Nat. Mater.* **2005**, *4*, 455-459.

70. Law, M.; Greene, L. E.; Radenovic, A.; Kuykendall, T.; Liphardt, J.; Yang, P. D. *J. Phys. Chem. B* **2006**, *110*, 22652-22663.

71. Beermann, N.; Vayssieres, L.; Lindquist, S. E.; Hagfeldt, A. *J. Electrochem. Soc.* **2000**, *147*, 2456-2461.

72. Erné, B. H.; Vanmaekelbergh, D.; Kelly, J. J. *J. Electrochem. Soc.* **1996**, *143*, 305-314.

73. Erné, B. H.; Vanmaekelbergh, D.; Kelly, J. J. *Adv. Mater.* **1995**, *7*, 739-742.

74. Goodey, A. P.; Eichfeld, S. M.; Lew, K. K.; Redwing, J. M.; Mallouk, T. E. *J. Am. Chem. Soc.* **2007**, *129*, 12344-+.

75. Dalchiele, E. A.; Martín, F.; Leinen, D.; Marotti, R. E.; Ramos-Barrado, J. R. *J. Electrochem. Soc.* **2009**, *156*, K77-K81.